発表者氏名	論文タイトル名	発表誌名	巻号	ページ	出版年
安藤秀二	最近の輸入発疹熱事例について	人と動物の共通感染症研究会のニューズレター	10	4-6	2011
岸本壽男	リケッチア症の新たな展開	感染・炎症・免疫	41(2)	62-64	2011
川上万里、梅川康弘、田原研司、木田浩司、藤井理津志、岸本壽男	日本紅斑熱の1例：岡山県初事例	肝臓	51(12)	714-721	2010
岸本壽男、木田浩司	リケッチア感染症の現状と課題	感染症	41(5)	157-168	2011
岸本　壽男、木田浩司、葛谷光隆、浜野雅子、藤井理津志	クラミジア、リケッチア	臨床と微生物	36（増刊号）	581-587	2009
高田伸弘、岸本壽男、岩崎博道、上田孝典、安藤秀二、大橋典男、矢野泰弘、田原研司、山内健生、藤田博己	ダニ関連細菌感染症、特にリケッチア症の新たな展開	感染症学雑誌	84（臨時増刊号）	138-143	2010

201123006A（別刷）

厚生労働科学研究費補助金
新型インフルエンザ等新興・再興感染症研究事業

リケッチアを中心としたダニ媒介性細菌感染症の総合的対策に関する研究

平成23年度　研究成果の刊行物・別刷

平成２４（２０１２）年3月

研究代表者　岸本　壽男
（岡山県環境保健センター）

厚生労働科学研究費補助金

新型インフルエンザ等新興・再興感染症研究事業

リケッチアを中心としたダニ媒介性細菌感染症の総合的対策に関する研究

平成２３年度　研究成果の刊行物・別刷

平成２４（２０１２）年3月

研究代表者　岸本　壽男

（岡山県環境保健センター）

発表者氏名	論文タイトル名	発表誌名	巻号	雑誌ページ	出版年	ページ
Murase Y, Konnai S, Hidano A, Githaka W.N, Ito T, Takano A, Kawabata H,Ato M, Tajima T,Tajima M,Onuma M, Murata S and Ohashi K.	Molecular detection of *Anaplasma phagocytophilum* in cattle and Ixodes persulcatus ticks.	Vet. Microbiol.	149	504-507	2011	1
Matsumura T, Ato M, Ikebe T, Ohnishi M, Watanabe H, Kobayashi K.	Interferon-γ-producing immature myeloid cells confer protection against severe invasive group A Streptococcus infections.	Nat. Commun.	3	678	2012	5
Gaowa, Wuritu, Wu, D., Yoshikawa, Y., Ohashi, N., Kawamori, F., Sugiyama, K., Ohtake, M., Ohashi, M., Yamamoto, S., Kitano, T., Takada, N., Kawabata, H.	Detection and characterization of p44/msp2 transcript variants of *Anaplasma phagocytophilum* from naturally infected ticks and wild deer in Japan	Jpn. J. Infect. Dis.	65	79-83	2012	16
Matsumoto, K., Takeuchi, T., Yokoyama, N., Katagiri, Y., Ooshiro, M., Zakimi, S., Gaowa, Kawamori, F., Ohashi, N., Inokuma, H.	Detection of the new *Ehrlichia* species closely related to *Ehrlichia ewingii* from *Haemaphysalis longicornis* in Yonaguni Island, Okinawa, Japan	J. Vet. Med. Sci.	73	1485-1488	2011	21
Sen, E., Uchijima, Y., Kadosaka, T., Ohashi, N., Okamoto, Y., Fukui, T., and Masuzawa, T.	Molecular detection of *Anaplasma phagocytophilum* and *Borrelia burgdorferi* in *Ixodes ricinus* ticks from Istanbul metropolitan area and rural Trakya (Thrace) region of Northwestern Turkey	Ticks Tick Borne Dis.	2	94-98	2011	25
Uchiyama, T., Kishi, M., and Ogawa, M.	Restriction of the growth of a nonpathogenic spotted fever group rickettsia	FEMS Immunology and Medical Microbiology	64(1)	42-47	2012	30
Uchiyama, T., Ogawa, M., Kishi, M., Yamashita, T., Kishimoto, T., and Kurane, I.	Restriction of the growth of typhus group rickettsiae in tick cells	Clinical Microbiology and Infection	15 (Suppl.2)	332-333	2009	36
Ogawa, M., Shinkai-Ouchi, F., Uchiyama, T., Hagiwara, K., Hanada, K., Kurane, I, and Kishimoto, T.	Shotgun proteomics of *Orientia tsutsugamushi*	Clinical Microbiology and Infection	15 (Suppl.2)	239-240	2009	38
Chan, Y.G.Y., Cardwell, M.M., Hermanas, T.M., Uchiyama, T., and Martinez, J.J.	Rickettsial outer-membrane protein B (rOmpB) mediates bacterial invasion through Ku70 in an actin, c-Cbl, clathrin and caveolin 2-dependent manner	Cellular Microbiology	11(4)	629-644	2009	40
冨岡鉄平、島田智恵、藤本嗣人、松井珠乃、佐藤弘、八幡祐一郎、橘とも子、岡部信彦	日本紅斑熱発生地域および近隣の発生が少ない地域における知識および受診行動	感染症学雑誌	85	180-183	2011	56
松井珠乃, 藤本嗣人, 佐藤弘, 安井良則, 岡部信彦	つつが虫病および日本紅斑熱について発生頻度が異なる地域での市民医学講座参加者における認知度比較	感染症学雑誌	84(1)	48-51	2010	60
Matsui T, Kobayashi J, Satoh H, Fujimoto T, Okabe N, Ando S, Kishimoto T, Yamamoto S.	Surveillance, recognition, and reporting of Tsutsugamushi disease (scrub typhus) and Japanese spotted fever by general practice clinics in Miyazaki Prefecture, determined by questionnaire survey in 2007	J Infect Chemother.	15(4)	269-272	2009	64

発表者氏名	論文タイトル名	発表誌名	巻号	雑誌ページ	出版年	ページ
Fujisawa T, Kadosaka T, Fujita H, Ando S, Takano A, Ogasawara Y, Kawabata H, Seishima M.	*Rickettsia africae* Infection in a Japanese Traveller with Many Tick Bites.	Acta Dermato-Venereologica.			(In press)	68
Tamakuma K,Mizutani Y, Inada K,Miyamoto K, Utsunomiya H,Mahara F, Tsutsumi Y ほか2名	Histopathological diagnosis of Japanese spotted fever using formalin-fixed, paraffin-embedded skin biopsy specimens Usefulness of Immunohistochemistry and real-time PCR analysis	Clin Microbiol Infect	Available on line		2011	70
玉熊桂子, 堤 寛	リアルタイムPCRによるホルマリン固定パラフィン包埋標本からの *Rickettsia japonica* DNAの検出:基礎的検討	藤田学園医学会誌	35(1)	25-27	2011	78
馬原文彦、藤田博己	野生動物と動物由来感染症:つつが虫病と日本紅斑熱	公衆衛生	75(1)	31-35	2011	81
Shiogama K, Mizutani Y, Inada K, Tsutsumi Y, ほか5名	Hepatitis C virus infection in a Japanese leprosy sanatorium for the past 67 years	J Med Virol	82	556-561	2010	86
堤 寛	劇症型感染症の病理	法医病理	16	69-82	2010	92
堤 寛	感染症における病理診断の役割	病理と臨床	28(4)	360-366	2010	106
馬原文彦	感染症法と保険診療:日本紅斑熱、つつが虫病の臨床と保険診療の課題	医学のあゆみ	232(8)	867-870	2010	113
馬原文彦	感染症法と保険診療:感染症法第四類感染症の検査、治療薬の保険適用について	医学のあゆみ	231(12-13)	1185-1186	2009	117
高田伸弘	医ダニ類の形態と病害	モダンメディア	57(6)	185-188	2011	119
高田伸弘	病気のはなし -最近のリケッチア症-	検査と技術	39(4)	262-268	2011	123
Takano, A., Nakao, M., Masuzawa, T., Takada, N., Yano, Y., Ishiguro, F., Fujita, H., Ito, T., Ma, X., Oikawa, Y., Kawamori, F., Kumagai, K., Mikami, T., Hanaoka, N., Ando, S., Honda, N., Taylor, K., Tsubota, T., Konnai, S., Watanabe, H., Ohnishi, M. and Kawabata, H.	Multilocus sequence typing implicates rodents as the main reservoir host of human-pathogenic *Borrelia garinii* in Japan.	Journal of Clinical Microbiology	49(5)	2035-2039	2011	130
岸本壽男	リケッチア症の新たな展開	感染・炎症・免疫	41(2)	62-64	2011	135
川上万里、梅川康弘、田原研司、木田浩司、藤井理津志、岸本壽男	日本紅斑熱の1例:岡山県初事例	肝臓	51(12)	714-721	2010	138
岸本壽男、木田浩司	リケッチア感染症の現状と課題	感染症	41(5)	157-168	2011	146
岸本壽男、木田浩司、葛谷光隆、浜野雅子、藤井理津志	クラミジア、リケッチア	臨床と微生物	36(増刊号)	581-587	2009	158

発表者氏名	論文タイトル名	発表誌名	巻号	雑誌ページ	出版年	ページ
高田伸弘、岸本壽男、岩崎博道、上田孝典、安藤秀二、大橋典男、矢野泰弘、田原研司、山内健生、藤田博己	ダニ関連細菌感染症、特にリケッチア症の新たな展開	感染症学雑誌	84(臨時増刊号)	138-143	2010	165

Veterinary Microbiology 149 (2011) 504–507

Contents lists available at ScienceDirect

Veterinary Microbiology

journal homepage: www.elsevier.com/locate/vetmic

Short communication

Molecular detection of *Anaplasma phagocytophilum* in cattle and *Ixodes persulcatus* ticks

Yusuke Murase [a,1], Satoru Konnai [a,1], Arata Hidano [a], Naftali W. Githaka [a], Takuya Ito [b], Ai Takano [c], Hiroki Kawabata [c], Manabu Ato [c], Tomoko Tajima [d], Motoshi Tajima [e], Misao Onuma [a], Shiro Murata [a], Kazuhiko Ohashi [a,*]

[a] Department of Disease Control, Graduate School of Veterinary Medicine, Hokkaido University, Sapporo 060-0818, Japan
[b] Hokkaido Institute of Public Health, Sapporo, 060-0819, Japan
[c] National Institute of Infectious Diseases, Toyama 1-23-1, Shinjuku-ku, Tokyo 162-8640, Japan
[d] Course of Veterinary Science, Graduate School of Life and Environmental Science, Osaka Prefecture University, Izumisano 598-8531, Japan
[e] Veterinary Teaching Hospital, Graduate School of Veterinary Medicine, Hokkaido University, Sapporo 060-0818, Japan

ARTICLE INFO

Article history:
Received 8 July 2010
Received in revised form 15 November 2010
Accepted 17 November 2010

Keywords:
Anaplasma phagocytophilum
Cattle
Tick

ABSTRACT

The tick-borne pathogen, *Anaplasma phagocytophilum* (*A. phagocytophilum*), the causative agent of human granulocytic anaplasmaposis (HGA), is increasingly becoming a public health concern as an aetiological agent for emerging infectious disease. We found *A. phagocytophilum* infection in a pooled sample of field-collected *Ixodes persulcatus* (*I. persulcatus*) ticks from one district in Hokkaido, Japan. Thus, to further investigate the prevalence in field-collected ticks, we used PCR assays targeting the *A. phagocytophilum* gene encoding 44 kDa major outer membrane protein (*p44*) for screening of *I. persulcatus* ticks and samples from cattle from pastures. Out of the 281 *I. persulcatus* ticks, 20 (7.1%) were found to harbor *A. phagocytophilum* DNA. The infection rate for *A. phagocytophilum* in cattle was 3.4% (42/1251). In future studies, it will be necessary to investigate effects of the infection in order to understand its pathogenesis of *A. phagocytophilum* in domestic animals.

1. Introduction

Anaplasma phagocytophilum (*A. phagocytophilum*) is a tick-borne obligate intracellular bacterium that infects the granulocytes of various mammals, including humans, sheep, goats, horses, dogs, cattle, llamas, and rodents, and first was identified as a human pathogen in 1994 (Chen et al., 1994; Dumler et al., 2005). Clinical symptoms include pyrexia, headache, respiratory symptoms and gastrointestinal symptoms in humans, and abortion, pyrexia and edema in cattle (Chen et al., 1994; Petrovec et al., 1997; Woldehiwet, 2006). Ixodes ticks are the main vector hosts of *A. phagocytophilum*, with *Ixodes scapularis* (*I. scapularis*) and *I. pacificus* harbouring the pathogen in USA, *I. ricinus* in Europe and *I. persulcatus* in Russia and Japan (Piesman and Eisen, 2008). In Japan, previous studies have reported the presence of *A. phagocytophilum* from reservoirs and vectors (Inokuma et al., 2007; Kawahara et al., 2006; Ohashi et al., 2005; Wuritu et al., 2009). In the present study, we have assessed the prevalence of *A. phagocytophilum* infections in ticks and cattle in the central area of Hokkaido by molecular epidemiological methods.

2. Materials and methods

2.1. Detection of *A. phagocytophilum* in ticks

Host-seeking Ixodes adult ticks were collected by flagging with cotton flannel at the central area of Hokkaido,

* Corresponding author at: Department of Disease Control, Graduate School of Veterinary Medicine, Hokkaido University, Sapporo, 060-0818, Japan. Tel.: +81 11 706 5215; fax: +81 11 706 5217.
E-mail address: okazu@vetmed.hokudai.ac.jp (K. Ohashi).
[1] The first two authors contributed equally to the report.

0378-1135/$ – see front matter.
doi:10.1016/j.vetmic.2010.11.025

Japan, as described previously (Konnai et al., 2008). The ticks were transported alive to the laboratory and mechanically disrupted using pipette tips to extract DNA. As preliminary survey, a pooled salivary gland sample of *I. persulcatus* ticks (15 female ticks) was used for the detection of *A. phagocytophilum* by PCR. PCR was performed by using primers MSP2-3F (5′-CCA GCG TTT AGC AAG ATA AGA G-3′) and MSP2-3R (5′-GCC CAG TAA CAA CAT CAT AAG C-3′) as described previously (Massung and Slater, 2003; Zeidner et al., 2000), which can specifically amplify a 334 bp portion of the *p44* gene of *A. phagocytophilum*. To further investigate the prevalence of *A. phagocytophilum* in ticks, a total of 325 unfed, host-seeking *I. persulcatus* and *I. ovatus* ticks were collected from the same area, and individually analyzed for the presence of *A. phagocytophilum* DNA. The detection of *A. phagocytophilum* was conducted using 150 ng of purified DNA under the same PCR condition described above. To determine the presence of DNA in the samples, PCR amplification of the tick actin gene was performed using a specific primer set (5′-TGG ATC GGC GGC TCC ATC CT-3′, and 5′-GAA GCA CTT GCG GTG GAC AAT G-3′), as previously described (Konnai et al., 2006).

2.2. Tested cattle

A total of 1251 bovine samples used for the detection of *A. phagocytophilum* were obtained from the Veterinary Teaching Hospital, Graduate School of Veterinary Medicine, Hokkaido University (Sapporo, Japan) as aliquots of DNA samples were used for the diagnostic tests for bovine leukemia virus. All of the cattle for sampling were from grazing pastures in the same district where *A. phagocytophilum*-infected ticks were found. Each bovine blood sample was taken within one year before/after *A. phagocytophilum* was detected in the ticks. Genomic DNA was extracted from 0.5 ml of whole blood samples using the Wizard™ genomic DNA kit (Promega Corp., Madison, WI, USA) according to the manufacturer's instructions. The detection of *A. phagocytophilum* was conducted using 150 ng of purified DNA under the same PCR conditions described above. To determine the presence of DNA in the samples, PCR amplification of the bovine β-globin gene was performed using a specific primer set, PCO3 (5′-ACA CAA CTG TGT TCA CTA GC-3′) and PCO4 (5′-CAA CTT CAT CCA CGT TCA CC-3′), as previously described (Konnai et al., 2006).

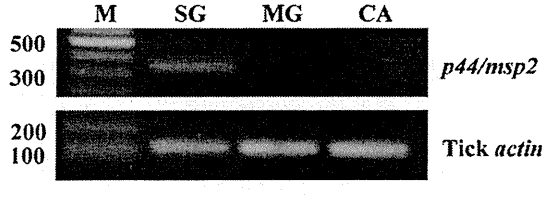

Fig. 1. Detection of *A. phagocytophilum* in different tissues of ticks. Predicted sizes of *A. phagocytophilum p44* and tick *actin* genes are 334 bp and 108 bp, respectively. The 100 bp molecular weight marker is in lane M. Salivary gland (SG), Midgut (MG) and Carcass (CA) (remnants after removal of SG and MG) were collected from 15 adult *I. persulcatus* female ticks.

Table 1
Detection of *A. phagocytophilum* in field-collected tick.

Species	No. tested	No. positive
I. persulcatus		
Male	155	13 (8.4%)
Female	126	7 (5.6%)
(Total)	281	20 (7.1%)
I. ovatus		
Male	19	0 (0%)
Female	25	0 (0%)
(Total)	44	0 (0%)
Total	325	20 (6.2%)

3. Results

3.1. Detection of A. phagocytophilum in field collected ticks

As preliminary survey, the detection of *A. phagocytophilum* infection was performed by a PCR method using pooled samples. As shown in Fig. 1, *A. phagocytophilum* was specifically detected in salivary glands of adult ticks, but not in midguts and tick carcasses. Thus, to further investigate the prevalence of *A. phagocytophilum* in ticks, a total of 325 unfed, host-seeking *I. persulcatus* and *I. ovatus* ticks were collected from the same area, and individually analyzed for the presence of *A. phagocytophilum* DNA (Table 1). Overall, among the *I. persulcatus* ticks, 7.1% (20/281) were found to be infected with *A. phagocytophilum*. The infection rates were 5.6% (7/126) and 8.4% (13/155) in female and male ticks, respectively. In this study, *A.*

Table 2
Detection of *A. phagocytophilum* in cattle.

Herd no.	No. tested	No. positive
A	7	1 (14.3%)
B	11	0 (0%)
C	34	1 (2.9%)
D	14	1 (7.1%)
E	3	0 (0%)
F	18	1 (5.6%)
G	9	0 (0%)
H	13	1 (7.7%)
I	17	0 (0%)
J	10	1 (10.0%)
K	125	7 (5.6%)
L	14	0 (0%)
M	20	0 (0%)
N	5	0 (0%)
O	11	0 (0%)
P	12	0 (0%)
Q	2	0 (0%)
R	18	0 (0%)
S	10	0 (0%)
T	1	0 (0%)
U	1	0 (0%)
V	31	1 (3.2%)
W	42	1 (7.1%)
X	424	14 (3.3%)
Y	324	9 (2.8%)
Z	45	2 (4.4%)
AA	30	0 (0%)
Total	1251	42 (3.4%)

phagocytophilum was not detected from the 44 of *I. ovatus* ticks, although the number of samples tested was limited. The tick actin gene was amplified to check the integrity of the template DNA and could be detected among all the ticks sampled (data not shown).

3.2. Prevalence of *A. phagocytophilum* infection in cattle from the district where infected ticks were detected

A total of 1,251 cattle from various sizes of herds were individually analyzed for the presence of *A. phagocytophilum* DNA (Table 2). Of the 1251 cattle DNA samples analyzed, 42 (3.4%) were positive for *A. phagocytophilum*, although the infection rates were different among the herds (0–14.3%).

4. Discussion

The objectives of the present study were to assess the prevalence of *A. phagocytophilum* in cattle and ticks. In previous studies, molecular survey was conducted for *I. persulcatus* and *I. ovatus* in Honshu, Japan. In Hokkaido, however, molecular survey was mainly conducted for *Haemophysalis* ticks. In this study, *A. phagocytophilum* was found to be prevalent in *I. persulcatus* ticks (7.2%) in the surveyed area. In this surveillance, *A. phagocytophilum* was not detected in *I. ovatus* ticks, although the number of ticks tested was limited. In Japan, *A. phagocytophilum* has also been detected in *I. ovatus* ticks (Ohashi et al., 2005). Thus, further investigation on the prevalence of *A. phagocytophilum* in Ixodes ticks including *I. ovatus* is needed. Recently, *A. phagocytophilum* was detected from larval ticks (Yoshimoto et al., 2010). There were many reports about the prevalence in adult ticks, but few reports on nymphal and larval ticks, and further investigation in nymphal and larval ticks is also needed to reveal the risk for the public health.

A. phagocytophilum-infected ticks were mainly collected from lower vegetation at the peripheral and inner parts of grazing lands for dairy and beef cattle, suggesting the possibility that the ticks could transmit the pathogen to cattle or had become infected after feeding on these cattle. To investigate this possibility, we examined the prevalence of *A. phagocytophilum* infections in cattle from the areas where *A. phagocytophilum* had been detected in the ticks. In this study, the infection rate of cattle with *A. phagocytophilum* was about 3.5% (42/1251), which was consistent with a previous report on the prevalence of *A. phagocytophilum* in cattle (1%, 1/78) at another area within Hokkaido (Jilintai et al., 2009). In Hokkaido, 10% of wild deer (*Cervus nippon yesoensis*) collected at 1975, 1989, and 1991 were infected with *A. phagocytophilum* (Kawahara et al., 2006), while 46% of deer collected at 2006 and 2007 were infected (Jilintai et al., 2009). These findings raise the possibility that, in Japan, *A. phagocytophilum* could be more widely distributed to domestic animals via ticks from wild animals than previously thought. *A. phagocytophilum* is the aetiological agent for tick-borne fever characterized by generalized edema and abortions in domestic ruminants (Woldehiwet, 2010). In our study, however, among the animals found to be infected, no specific disease symptoms were observed upon clinical examination, that is consistent with a previous study (Jilintai et al., 2009). In future studies, it will be necessary to investigate effects of the infection in order to understand its pathogenesis of *A. phagocytophilum* in domestic animals. On the other hand, *A. phagocytophilum* is also known as the causative agent of HGA, an emerging febrile disease. Since 1994, there has been an upswing in reported cases of the disease in the US, partly because of improved detection methods of the pathogen. Indeed, HGA is only second to Lyme disease as a tick-borne zoonosis in the US, and it is important to establish the extent of prevalence and distribution of this pathogen in Japan. Although the occurrence of HGA is still unknown in Japan including Hokkaido, the overall infection rate (3.5% in cattle and 7.1% in ticks) might indicate a potential public health risk of HGA in the studied area. Furthermore, it would be interesting to determine the level of virulence of the Hokkaido isolates of *A. phagocytophilum*.

5. Conclusions

Although our study determined low prevalence rates among ticks collected from the sampling sites, the detection of infected cattle from the same areas indicates that these ticks are highly efficient in transmission of *A. phagocytophilum*, a significant finding given that this pathogen is zoonotic. Studies utilizing larger sample size and from different geographical regions would provide further insight on the transmission dynamics of *A. phagocytophilum* in these areas.

Acknowledgements

The vital information given by Prof. Hisashi Inokuma of Obihiro University of Agriculture and Veterinary Medicine, Japan, is gratefully appreciated. We are indebted to Prof. Yasuko Rikihisa, Ohio State University, for donating the control DNA, and Dr. William Harold Witola for the help in preparing the manuscript. This work was supported by grants-in-Aid for Scientific Research from the Japan Society for the Promotion of Science (JSPS), a grant for the Global COE (Centers of Excellence) Program through the Hokkaido University and by a special grant for the Promotion of Basic Research Activities for Innovative Biosciences from the Bio-oriented Technology Research Advancement Institution (BRAIN).

References

Chen, S.M., Dumler, J.S., Bakken, J.S., Walker, D.H., 1994. Identification of a granulocytotropic *Ehrlichia* species as the etiologic agent of human disease. J. Clin. Microbiol. 32, 589–595.

Dumler, J.S., Choi, K.S., Garcia-Garcia, J.C., Barat, N.S., Scorpio, D.G., Garyu, J.W., Grab, D.J., Bakken, J.S., 2005. Human granulocytic anaplasmosis and *Anaplasma phagocytophilum*. Emerg. Infect. Dis. 11, 1828–1834.

Inokuma, H., Makino, T., Kabeya, H., Nogami, S., Fujita, H., Asano, M., Inoue, S., Maruyama, S., 2007. Serological survey of *Ehrlichia* and Anaplasma infection of feral raccoons (Procyon lotor) in Kanagawa Prefecture Japan. Vet. Parasitol. 145, 186–189.

Jilintai, Seino, N., Hayakawa, D., Suzuki, M., Hata, H., Kondo, S., Matsumoto, K., Yokoyama, N., Inokuma, H., 2009. Molecular survey for *Anaplasma bovis* and *Anaplasma phagocytophilum* infection in cattle

in a pastureland where sika deer appear in Hokkaido, Japan. Jpn. J. Infect. Dis. 62, 73–75.
Kawahara, M., Rikihisa, Y., Lin, Q., Isogai, E., Tahara, K., Itagaki, A., Hiramitsu, Y., Tajima, T., 2006. Novel genetic variants of *Anaplasma phagocytophilum*, *Anaplasma bovis*. Anaplasma centrale, and a novel *Ehrlichia* sp. in wild deer and ticks on two major islands in Japan. Appl. Environ. Microbiol. 72, 1102–1109.
Konnai, S., Imamura, S., Nakajima, C., Witola, W.H., Yamada, S., Simuunza, M., Nambota, A., Yasuda, J., Ohashi, K., Onuma, M., 2006. Acquisition and transmission of *Theileria parva* by vector tick, *Rhipicephalus appendiculatus*. Acta Trop. 99, 34–41.
Konnai, S., Saito, Y., Nishikado, H., Yamada, S., Imamura, S., Mori, A., Ito, T., Onuma, M., Ohashi, K., 2008. Establishment of a laboratory colony of taiga tick *Ixodes persulcatus* for tick-borne pathogen transmission studies. Jpn. J. Vet. Res. 55, 85–92.
Massung, R.F., Slater, K.G., 2003. Comparison of PCR assays for detection of the agent of human granulocytic ehrlichiosis. Anaplasma phagocytophilum. J. Clin. Microbiol. 41, 717–722.
Ohashi, N., Inayoshi, M., Kitamura, K., Kawamori, F., Kawaguchi, D., Nishimura, Y., Naitou, H., Hiroi, M., Masuzawa, T., 2005. *Anaplasma phagocytophilum*-infected ticks, Japan. Emerg. Infect. Dis. 11, 1780–1783.
Petrovec, M., Lotric Furlan, S., Zupanc, T.A., Strle, F., Brouqui, P., Roux, V., Dumler, J.S., 1997. Human disease in Europe caused by a granulocytic *Ehrlichia* species. J. Clin. Microbiol. 35, 1556–1559.
Piesman, J., Eisen, L., 2008. Prevention of tick-borne diseases. Annu. Rev. Entomol. 53, 323–343.
Woldehiwet, Z., 2006. *Anaplasma phagocytophilum* in ruminants in Europe. Ann. N Y Acad. Sci. 1078, 446–460.
Wuritu, Gaowa, Kawamori, F., Aochi, M., Masuda, T., Ohashi, N., 2009. Characterization of *p44*/msp2 multigene family of *Anaplasma phagocytophilum* from two different tick species *Ixodes persulcatus* and *Ixodes ovatus*, in Japan. Jpn. J. Infect. Dis. 62, 142–145.
Yoshimoto, K., Matsuyama, Y., Matsuda, H., Sakamoto, L., Matsumoto, K., Yokoyama, N., Inokuma, H., 2010. Detection of *Anaplasma bovis* and *Anaplasma phagocytophilum* DNA from *Haemaphysalis megaspinosa* in Hokkaido, Japan. Vet. Parasitol. 168, 170–172.
Zeidner, N.S., Burkot, T.R., Massung, R., Nicholson, W.L., Dolan, M.C., Rutherford, J.S., Biggerstaff, B.J., Maupin, G.O., 2000. Transmission of the agent of human granulocytic ehrlichiosis by *Ixodes spinipalpis* ticks: evidence of an enzootic cycle of dual infection with *Borrelia burgdorferi* in Northern Colorado. J. Infect. Dis. 182, 616–619.
Woldehiwet, Z., 2010. The natural history of *Anaplasma phagocytophilum*. Vet. Parasitol. 167, 108–122.

nature COMMUNICATIONS

OPEN

ARTICLE

Received 14 Nov 2011 | Accepted 11 Jan 2012 | Published 14 Feb 2012

DOI: 10.1038/ncomms1677

Interferon-γ-producing immature myeloid cells confer protection against severe invasive group A *Streptococcus* infections

Takayuki Matsumura[1], Manabu Ato[1], Tadayoshi Ikebe[2], Makoto Ohnishi[2], Haruo Watanabe[2] & Kazuo Kobayashi[1]

Cytokine-activated neutrophils are known to be essential for protection against group A *Streptococcus* infections. However, during severe invasive group A *Streptococcus* infections that are accompanied by neutropenia, it remains unclear which factors are protective against such infections, and which cell population is the source of them. Here we show that mice infected with severe invasive group A *Streptococcus* isolates, but not with non-invasive group A *Streptococcus* isolates, exhibit high concentrations of plasma interferon-γ during the early stage of infection. Interferon-γ is necessary to protect mice, and is produced by a novel population of granulocyte–macrophage colony-stimulating factor-dependent immature myeloid cells with ring-shaped nuclei. These interferon-γ-producing immature myeloid cells express monocyte and granulocyte markers, and also produce nitric oxide. The adoptive transfer of interferon-γ-producing immature myeloid cells ameliorates infection in wild-type and interferon-γ-deficient mice. Our results indicate that interferon-γ-producing immature myeloid cells have a protective role during the early stage of severe invasive group A *Streptococcus* infections.

[1] Department of Immunology, National Institute of Infectious Diseases, 1-23-1 Toyama, Shinjuku-ku, Tokyo 162-8640, Japan. [2] Department of Bacteriology I, National Institute of Infectious Diseases, 1-23-1 Toyama, Shinjuku-ku, Tokyo 162-8640, Japan. Correspondence and requests for materials should be addressed to M.A. (email: ato@nih.go.jp).

Streptococcus pyogenes (group A *Streptococcus*; GAS) is one of the most common human pathogens. It causes a wide variety of infections, ranging from uncomplicated pharyngitis and skin infections to severe and even life-threatening manifestations such as streptococcal toxic shock syndrome (STSS) and necrotizing fasciitis. The mortality rates for STSS and necrotizing fasciitis are high (30–70%), even following prompt antibiotic therapy and debridement[1–4].

It is widely believed that myeloid cells including polymorphonuclear leukocytes (PMNs) have a central role in survival from GAS infections, and interferon (IFN)-γ is essential to full activation and proper function of PMNs. Notably, IFN-γ at the infection site is thought to be critical for protection; however, its increased systemic levels seem to be detrimental to survival after GAS infections[5]. Therefore, the appropriate regulation of cytokine-producing cells may be critical for survival and host defense against severe invasive GAS infections.

Myeloid cells with ring-shaped nuclei (ring cells) are present in the peripheral blood of patients with myeloproliferative diseases, but only rarely in healthy control subjects[6,7]. Ring cells are usually referred to as PMNs. However, not only Gr-1^{high} PMN-like ring cells, but also Gr-1^{low} mononuclear cell-like ring cells are present in the bone marrow, peripheral blood, and inflammatory infiltrates of mice[8]. Morphologically, a part of myeloid-derived suppressor cells (MDSCs) has ring-shaped nuclei[9,10]. MDSCs are potent suppressors of T-cell immunity, and their presence is associated with a poor clinical outcome in cancer. They are divided into 2 subtypes according to morphology and surface markers: Ly-6G$^-$ Ly-6C^{high} monocytic MDSCs and Ly-6G$^+$ Ly-6C^{low} granulocytic MDSCs[11,12]. Recent studies have demonstrated the considerable suppressive potential of MDSCs on T-cell immunity in autoimmune diseases, and also in chronic infections with intracellular pathogens, such as *Salmonella typhimurium*, *Candida albicans*, *Trypanosoma cruzi*, and *Toxoplasma gondii*[13]. However, the biological functions of ring cells in infectious diseases, and also the relationship between ring cells and MDSCs, remain largely unknown.

In the present study, IFN-γ-producing immature myeloid cells with ring-shaped nuclei (γIMCs), which originated from bone marrow precursor-like cells (BMPCs), are shown to be functionally and phenotypically distinct from MDSCs. We demonstrate that γIMCs have a protective role against severe invasive GAS infections, and possibly compensate for neutropenia.

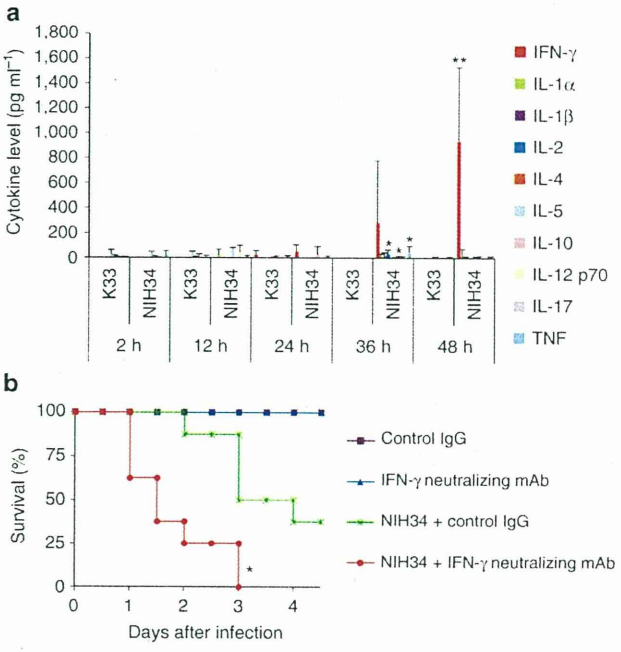

Figure 1 | IFN-γ is a host defense factor in mice infected with severe invasive GAS isolates. (**a**) C3H/HeN mice were i.p. inoculated with *S. pyogenes* (*emm3* genotype) clinical isolates (non-STSS, K33; STSS, NIH34; 3.0×10^7 CFU per mouse), and plasma cytokine levels were determined by FlowCytomix. Data are expressed as mean ± s.d. for at least 2 independent experiments, using a total of 6–10 mice for each group. The differences compared with K33-infected mice were statistically significant ($^*P<0.05$, $^{**}P<0.01$) as determined by Student's *t*-test. (**b**) C3H/HeN mice were i.p. inoculated with NIH34 (3.0×10^7 CFU per mouse) in the presence of an IFN-γ neutralizing mAb (clone R4-6A2) (1 mg per mouse) or control rat IgG (1 mg per mouse). Survival was observed for 4 days post-infection. Mortality differences compared with infected mice in the presence of control IgG were statistically significant ($^*P<0.05$), as determined by a log-rank test. Survival curves were generated from two independent experiments, using a total of eight mice for each group.

Results

Role of IFN-γ in severe invasive GAS infections. To clarify the types of cytokines involved in severe invasive GAS infections, we first investigated the dynamics of cytokines in severe invasive and non-invasive GAS infections. As a model of disseminated infection in normally sterile sites, we intraperitonially (i.p.) infected GAS-susceptible C3H/HeN mice[14–17] with either severe invasive (*emm3* genotype *rgg* gene-mutated STSS strain, NIH34) or non-invasive (*emm3* genotype non-STSS (pharyngitis) strain, K33) GAS clinical isolates[18], and measured the levels of plasma cytokines. We detected no significant amount of plasma cytokines within 24 h of infection. By contrast, in mice infected with severe invasive GAS isolates, but not with non-invasive GAS isolates, we detected high levels of plasma IFN-γ; moreover, the levels increased rapidly at 48 h post-infection (Fig. 1a). Other cytokines, such as IL-1α, IL-1β, IL-4, IL-5, IL-12 p70 and IL-17, were scarcely detected in the plasma of mice infected with either severe invasive or non-invasive isolates. By contrast, in mice infected with severe invasive GAS isolates, the levels of IL-2, IL-10, and TNF increased transiently at 36 h post-infection.

Further, we evaluated whether IFN-γ is the host factor contributing to protection against severe invasive GAS infections, or to deterioration of STSS through an augmented inflammatory process. We i.p. administered mice with an anti-mouse IFN-γ neutralizing mAb (clone R4-6A2), on the day of infection with severe invasive GAS isolates. At 72 h post-infection, all of the mice administered with the IFN-γ neutralizing mAb died. By contrast, 50% of the mice treated with rat IgG as a control survived (Fig. 1b). These results are consistent with those of a previous study[5], in which mice treated with a different IFN-γ neutralizing mAb (clone XMG1.2) and IFN-γ knockout (*Ifng*$^{-/-}$) mice were more susceptible to lethal skin infection with the M-nontypeable GAS strain 64/14 than were control IgG-administered mice and wild-type mice, respectively. Thus, IFN-γ may act as a host defense factor against severe invasive GAS infections.

A source of IFN-γ in severe invasive GAS infections. It is widely believed that T cells are a main source of IFN-γ in severe invasive GAS infections[19–21]. To identify the IFN-γ-producing cell types in mice infected with severe invasive GAS isolates, we used an *in vivo* intracellular cytokine synthesis (ICS) assay[22,23] to assess splenic IFN-γ production at 48 h post-infection. Unexpectedly, we revealed that Gr-1$^+$ CD11b$^+$ cells (but not TCR-β$^+$ TCR-γ/δ$^+$, CD4$^+$, or CD8$^+$ T cells, DX5$^+$ NK/NKT cells, or CD11c$^+$ MHC-II$^+$ dendritic cells) were a source of splenic IFN-γ in superantigen-insensitive C57BL/6 mice[24,25], and also in C3H/HeN mice (Fig. 2a and b). These Gr-1$^+$ cells appeared in the spleen on day 1 post-infection, subsequently increased in number, and were the major source of IFN-γ

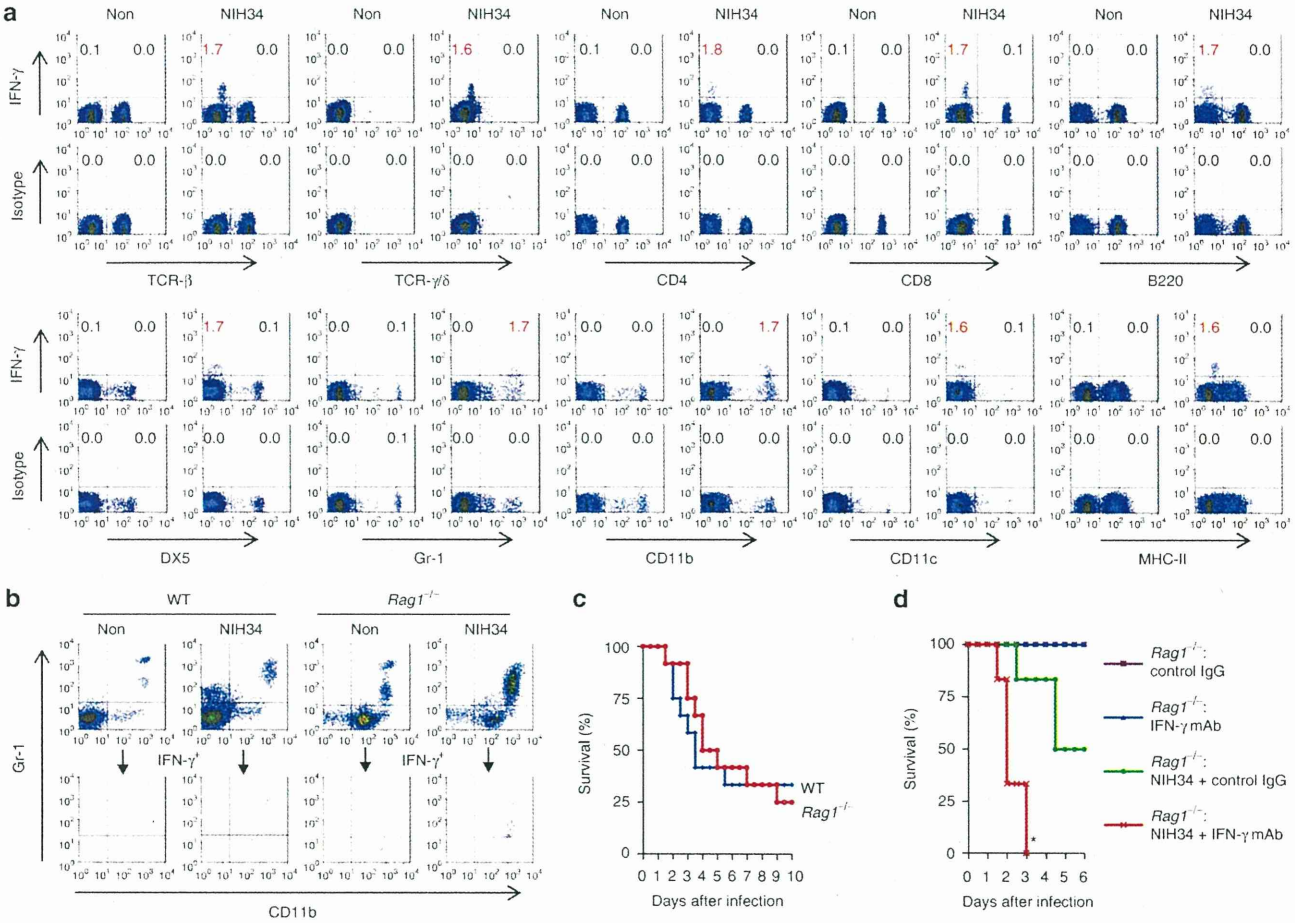

Figure 2 | CD11b$^+$ Gr-1$^+$ cells are the source of IFN-γ in severe invasive GAS infections. (**a**,**b**) C3H/HeN mice (**a**), C57BL per six mice (WT) (**b**), and *Rag1*$^{-/-}$ mice (**b**) with or without i.p. infection of NIH34 (3.0×10^7 CFU per mouse) for 42 h were i.v. injected with monensin. Six hours later, the mice were sacrificed and their splenocytes were immediately stained for the indicated markers, and analysed by ICS assay. (**a**) The numbers (%) in the plots represent the proportion of IFN-γ$^+$ subsets to total splenocytes. (**b**) Lower panels show the cells gated on the IFN-γ$^+$ population. Data are representative of three independent experiments. (**c**,**d**) WT and *Rag1*$^{-/-}$ mice were i.p. inoculated with NIH34 (3.0×10^7 CFU per mouse) in the absence (**c**) or presence (**d**) of an IFN-γ neutralizing mAb (clone R4-6A2) or control rat IgG (1 mg per mouse) as in Fig. 1b. Survival (in days) was observed as indicated. Survival curves were generated from 2 independent experiments, using a total of 12 mice for each group. (**d**) Mortality differences compared with infected mice in the presence of control IgG were statistically significant ($^*P<0.05$) as determined by a log-rank test.

throughout infection (Supplementary Fig. S1). By contrast, TCR-β$^+$ T cells and DX5$^+$ or NK1.1$^+$ NK cells, which are regarded as the sources of IFN-γ in GAS infections[15–17], produced small amounts of IFN-γ during the late stage (days 3–5 post-infection) of severe invasive GAS infections in C3H/HeN mice, but not in C57BL/6 mice. Notably, the accumulation of Gr-1$^+$ cells led to the clearance of infection from the spleen. Additionally, the administration of monensin, which blocks intracellular cytokine transport, did not induce spontaneous splenic production of IFN-γ (Fig. 2a and b; Supplementary Fig. S1).

To exclude the involvement of T cells in protection against severe invasive GAS infections, we investigated IFN-γ production in C57BL/6.RAG1 knockout (*Rag1*$^{-/-}$) mice, which have no mature B and T cells[26]. The ICS assay revealed that the cellular source of IFN-γ during severe invasive GAS infections was Gr-1$^+$ CD11b$^+$ cells in *Rag1*$^{-/-}$ mice, and also in C57BL/6 wild-type (WT) mice (Fig. 2b). We further examined the mortality of *Rag1*$^{-/-}$ mice during severe invasive GAS infections. We observed no significant difference in mortality between *Rag1*$^{-/-}$ and WT mice infected with severe invasive GAS isolates (Fig. 2c). Furthermore, similar to C3H/HeN mice (Fig. 1b), IFN-γ neutralizing mAb (clone R4-6A2)-treated *Rag1*$^{-/-}$ mice were more susceptible to severe invasive GAS infections than were control IgG-administered *Rag1*$^{-/-}$ mice (Fig. 2d). Our results indicate that mature B and T cells do not affect the mortality of infected mice, and that T cells have no protective effect during the early stage of severe invasive GAS infections.

Characterization of the early source of IFN-γ. Anti-Gr-1 mAb detects Ly-6C$^+$ monocytes and Ly-6G$^+$ PMNs. Therefore, to determine which subset of Gr-1$^+$ CD11b$^+$ cells is responsible for IFN-γ production during severe invasive GAS infections, we investigated the surface phenotype of IFN-γ-producing cells isolated from the spleens of mice at 48 h post-infection. The ICS assay revealed that IFN-γ-producing cells had the phenotype of monocytes (F4/80^{low} CX3CR1$^+$) and PMNs (Ly-6G$^+$ Ly-6C^{low}) (Fig. 3). Additionally, they expressed no lymphoid (CD27, IL-7Rα) or granulocyte-lineage (CCR3, Siglec-F, c-Kit, IL-5Rα (H7)) markers, but exhibited particular profiles of CCR2$^-$ CD31$^+$ CD34$^-$ CD38$^+$ CD44^{high} CD49d$^+$ CD62L$^+$ CD69$^+$ IL-5Rα (T21)^{high} Siglec-H$^-$ (Fig. 3; Supplementary Table S1). In this model, the most prominent GAS infection was present in the kidney[18,27]. In accordance with the bacterial burden in the peritoneal cavity, spleen and kidney, a higher proportion

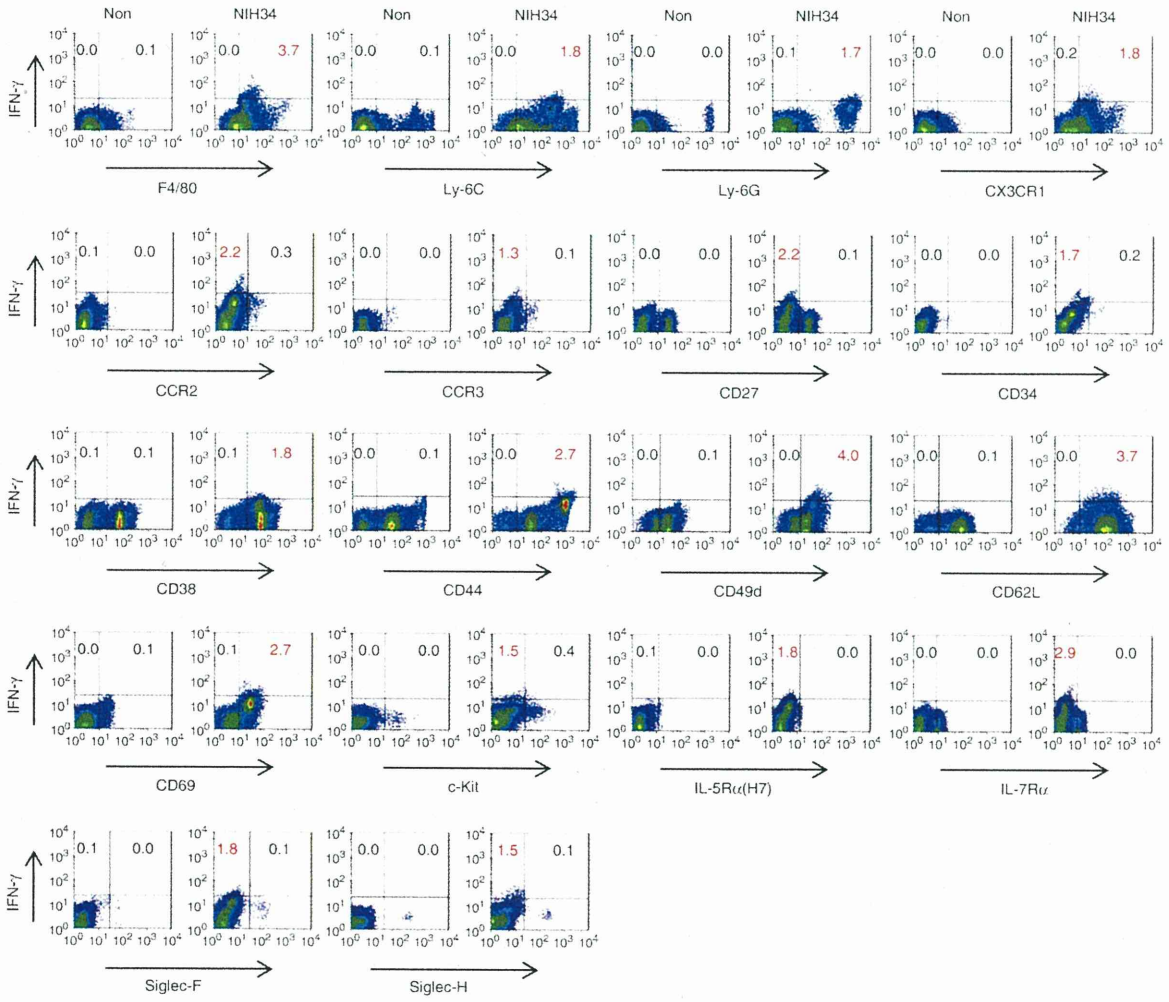

Figure 3 | IFN-γ-producing cells exhibit monocyte and PMN phenotypes in severe invasive GAS infections. C3H/HeN mice with or without i.p. infection of NIH34 (3.0×10^7 CFU per mouse) for 42 h were i.v. injected with monensin. Six hours later, the mice were killed and their splenocytes were immediately stained for the indicated markers, and analysed by the ICS assay. The numbers (%) in the plots represent the proportion of IFN-γ$^+$ subsets to total splenocytes. These data are representative of three independent experiments.

of IFN-γ-producing cells accumulated in the kidney of C3H/HeN mice, and also C57BL/6 mice i.p. infected with NIH34 (Supplementary Fig. S2). By contrast, lower proportion of IFN-γ-producing cells existed at the sites of infection. A skin-infection model yielded similar results (Supplementary Fig. S2). Furthermore, IFN-γ-producing cells were detected in the spleens from mice infected with various STSS strains[18,27] (Supplementary Fig. S3). These cells were also detected in the peripheral blood and (in particularly high frequency) the bone marrow from NIH34-infected mice (Fig. 4a–d; Supplementary Fig. S4). Interestingly, Siglec-F$^+$ eosinophils (Eos) stained with IL-5Rα (H7) and IL-5Rα (T21), whereas IFN-γ-producing cells stained well with T21, but not with H7 (Fig. 4e), suggesting that IFN-γ-producing cells were phenotypically distinct from Eos. IFN-γ-producing cells were also phenotypically distinct from Ly-6C^{low} CD31$^-$ PMNs (Fig. 4d). Moreover, the number and proportion of PMNs were markedly reduced in the spleen, peripheral blood, and bone marrow at 48 h post-infection (Fig. 4d and f), as reported in human STSS cases[28].

Immature myeloid cells as an early source of IFN-γ. The IFN-γ-producing cells expressed the phenotypic markers of monocytes/macrophages (F4/80 and CX3CR1) and PMNs (Ly-6G). Therefore, we sorted CD11b$^+$ CD11c$^-$ F4/80^{low} Ly-6G$^+$ cells from the spleens of infected mice and morphologically analysed them with May-Grünwald-Giemsa staining. The IFN-γ-producing CD11b$^+$ CD11c$^-$ F4/80^{low} Ly-6G$^+$ splenocytes were IMCs, but not monocytes/macrophages or PMNs. These IFN-γ-producing IMCs were large cells containing ring-shaped, non-segmented nuclei, with a coarse chromatin pattern[6–8] (Fig. 5a and b). The sorted cells were contaminated with a small number of PMNs; however, immunohistochemical analyses showed that IMCs, but not PMNs, were the source of IFN-γ (Fig. 5c). The cells with ring-shaped nuclei were also observed in the peritoneum, kidney, and spleen from i.p. infection model, and in the skin from subcutaneous (s.c.) infection model, whereas such cells were not observed in the spleen and kidney from non-infected or non-invasive K33 strain-infected mice (Fig. 5d and e). To determine whether IFN-γ-producing IMCs (γIMCs) are committed to the granulocyte or monocyte lineage, we cultured sorted CD11b$^+$ CD11c$^-$ F4/80^{low} Ly-6G$^+$ γIMCs *in vitro*, in the presence of G-CSF, M-CSF, GM-CSF or IL-5. We observed that G-CSF, M-CSF and IL-5 failed to promote differentiation and survival (Fig. 5f). By contrast, in the presence of GM-CSF, differentiated γIMCs increased their expression of CD11c, F4/80, DX5 and Siglec-F (Fig. 5g) with the polymorphonuclear phenotype (Fig. 5h). Such granulocyte-like cells showed

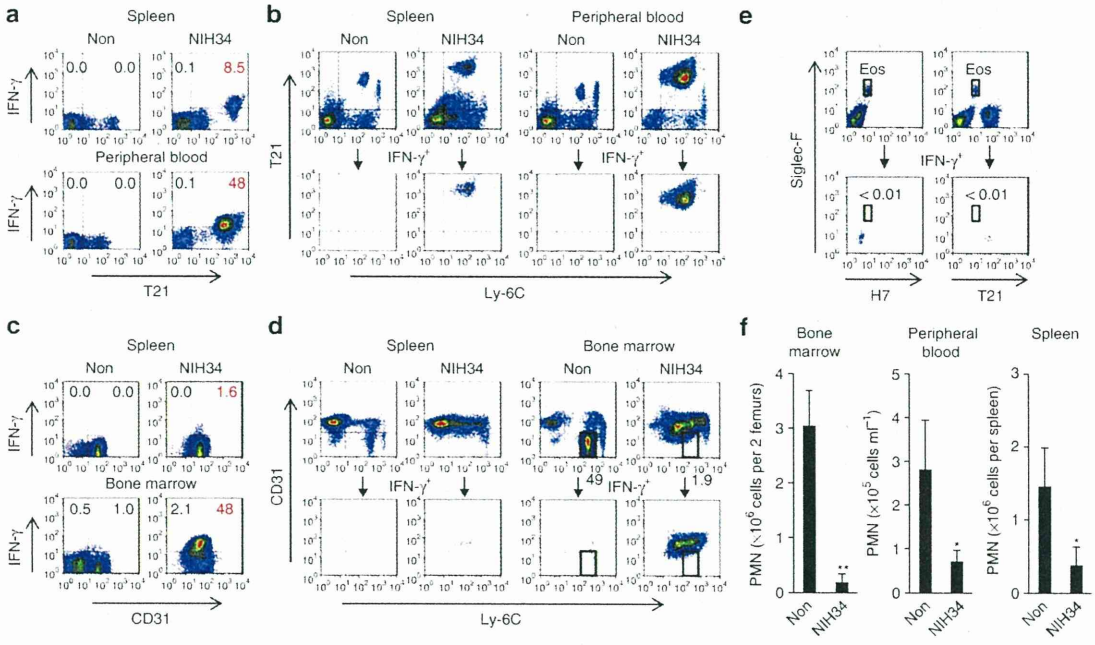

Figure 4 | IFN-γ-producing cells are detected in the peripheral blood and the bone marrow of GAS-infected mice. (**a**–**d**) Non-infected C3H/HeN mice or (**a**–**e**) mice i.p. infected with NIH34 (3.0×10^7 CFU per mouse) for 42 h were i.v. injected with monensin. Six hours later, the mice were killed and their splenocytes (**a**–**e**), peripheral blood cells (**a**,**b**), and bone marrow cells (**c**,**d**) were immediately stained for the indicated markers, and analysed by ICS assay. (**a**,**c**) The numbers (%) in the plots represent the proportion of IFN-γ$^+$ subsets to total cells. (**b**,**d**,**e**) Lower panels show the cells gated on the IFN-γ$^+$ population. (**d**,**e**) Rectangle gates in the plot represent mature granulocytes (**d**) and Eos (**e**). The numbers (%) in the plots represent the proportion of mature granulocytes (**d**) or IFN-γ$^+$ Eos (**e**) to total cells. Data are representative of three independent experiments. (**f**) The numbers of PMNs in the bone marrow, peripheral blood, and spleen from non-infected or NIH34-infected mice at 48 h. Data are expressed as mean ± s.d. ($n=3$). The differences compared with non-infected mice were statistically significant ($^*P<0.05$, $^{**}P<0.01$) as determined by Student's t-test.

reduced ability to produce IFN-γ (Fig. 5i), and were phenotypically different from c-Kit^{low} H7$^+$ Siglec-F$^+$ bone marrow-derived Eos and CCR3$^+$ H7$^+$ Siglec-F$^+$ splenic Eos[29]; (Supplementary Fig. S5). These results suggest that γIMCs are committed to the granulocyte lineage, but do not exist in the steady state, and produce IFN-γ during a specific stage of differentiation.

Nitric oxide (NO) is considered to be a main mechanism for controlling some infective agents. Myeloid cells are able to release NO in response to IFN-γ[30–33]; moreover, IFN-γ and NO-producing myeloid cells have been described in cancer[34]. Therefore, we investigated the ability of γIMCs to produce NO in response to GAS. When stimulated by autocrine and/or paracrine IFN-γ, γIMCs (but not than PMNs and granulocyte-like cells differentiated from γIMCs using GM-CSF) were able to produce NO, because their NO production was significantly blocked in the presence of IFN-γ neutralizing mAb (Fig. 5j).

Differentiation of precursor-like cells into γIMCs. Bone marrow contains the highest proportion of γIMCs (Fig. 4c and d). Therefore, we attempted to identify the precursors of γIMCs in the bone marrow of mice infected with severe invasive GAS isolates. Interestingly, analysis of the surface molecules revealed 2 distinct subsets of IFN-γ-producing cells (Fig. 6a): a minor and a major subset. The minor subset constituted 6.9 ± 3.2% of IFN-γ-producing bone marrow cells (Fig. 6b), and comprised CD11b$^+$ CD11c$^-$ F4/80^{low} Ly-6G$^+$ large cells (Supplementary Fig. S6), containing ring-shaped nuclei (BM-γIMCs) (Fig. 6c). On the basis of morphology and surface phenotype, these cells corresponded to splenic γIMCs (Sp-γIMCs) (Fig. 5a and b). Neither isolated BM-γIMCs nor Sp-γIMCs proliferated in the presence of GM-CSF (Figs 5f and 6d). These cells differed from metamyelocytes and immature neutrophils in non-infected bone marrow (Fig. 6c). The major subset of IFN-γ-producing cells comprised CD11b$^+$ CD11c^{low} F4/80$^+$ Ly-6G^{low} precursor-like cells (BMPCs) (Fig. 6b; Supplementary Fig. S6), which constituted 74.8 ± 13.7% of IFN-γ-producing cells (Fig. 6b). This subset consisted of ~10% monocyte-like ring cells and immature myeloid cells (Fig. 6c), which are phenotypically different from CD11b$^-$ Ly-6G$^-$ cells such as granulocyte–monocyte progenitors, common myeloid progenitors, and myelolymphoid progenitors[35]. In the presence of GM-CSF, isolated BMPCs proliferated (Fig. 6d) and differentiated into BM-γIMCs (Fig. 6c and e). Moreover, after 2 extra days of incubation with GM-CSF, differentiated BM-γIMCs increased their expression of CD11c, F4/80, DX5 and Siglec-F (Fig. 6f). The polymorphonuclear and cell surface phenotype (Supplementary Fig. S6) was similar to that of Sp-γIMCs cultured with GM-CSF (Fig. 5g and h). The differentiation of BMPCs into BM-γIMCs was totally blocked in the presence of IFN-γ neutralizing mAb; by contrast, this cytokine was dispensable for differentiation into granulocyte-like cells (Supplementary Fig. S6). These results are in accordance with the absence of Ly-6G$^+$ γIMCs in the spleen of GAS-infected C57BL6.*Ifng*$^{-/-}$ mice (Supplementary Fig. S7). The expression level of Ly-6G in PMNs was similar for WT and *Ifng*$^{-/-}$ mice (Supplementary Fig. S7). As with γIMCs and γIMC-differentiated granulocyte-like cells (Fig. 5i), the cells differentiated from BMPCs, after 2 extra days of incubation with GM-CSF, retained the ability to release IFN-γ in response to GAS; however, subsequent differentiation by GM-CSF reduced the ability to produce IFN-γ (Fig. 6g). A few IFN-γ-producing cells in non-infected mice were recognized in the same fraction as the BMPCs (Fig. 6a), and, therefore, it is possible that BMPCs exist in the naïve bone marrow. Our results suggest that IFN-γ-producing BMPCs are the precursors of γIMCs, and that their differentiation is dependent on autocrine and/or paracrine pathways involving

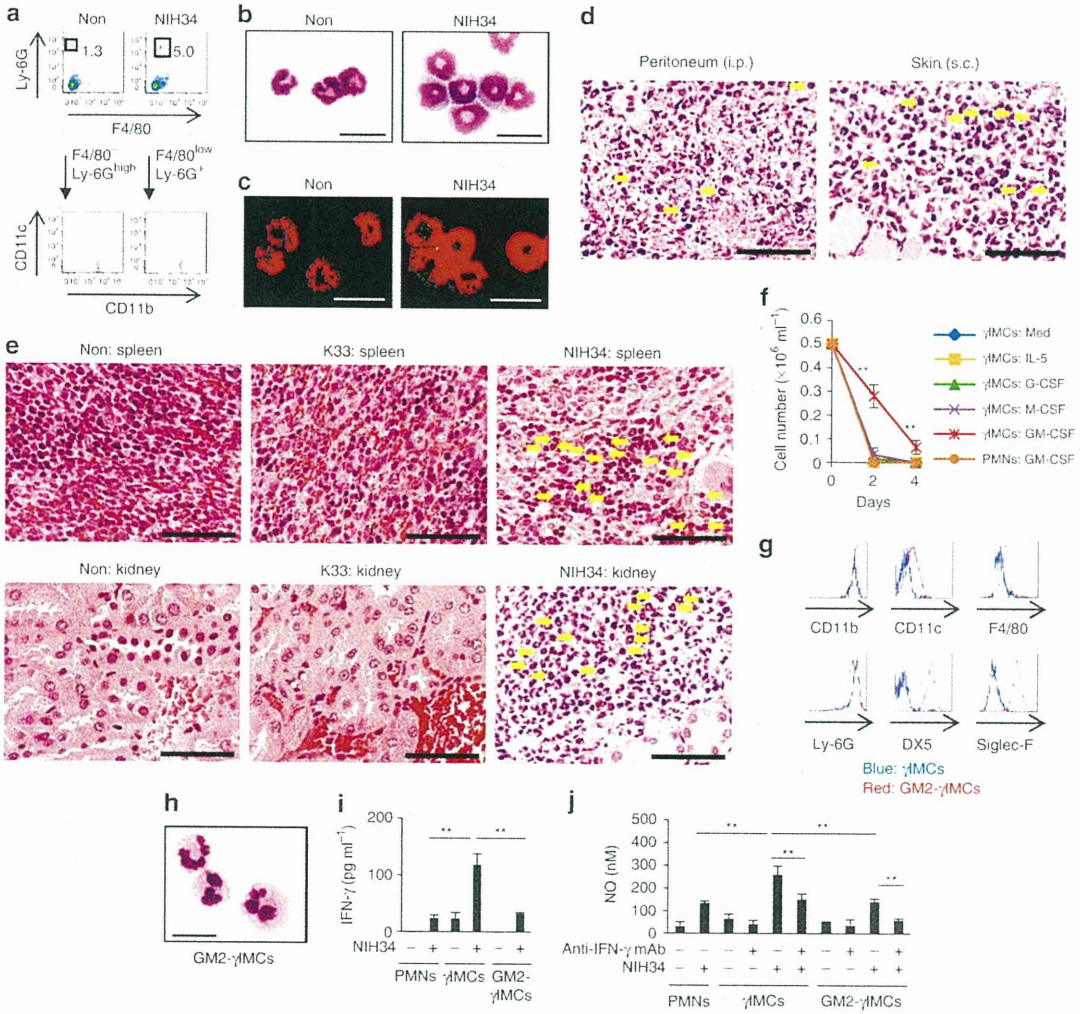

Figure 5 | γIMCs are the source of IFN-γ in severe invasive GAS infections. (**a**) CD11b$^+$ CD11c$^-$ F4/80$^-$ Ly-6G^{high} PMNs in splenocytes from non-infected C3H/HeN mice, or CD11b$^+$ CD11c$^-$ F4/80^{low} Ly-6G$^+$ γIMCs in splenocytes from mice infected with NIH34, were isolated by FACS. (**b**,**c**) Cytospin preparations of each sorted cell type were visualized with May-Grünwald-Giemsa staining (**b**), whereas intracellular IFN-γ (green, IFN-γ; red, nuclei) was visualized with a confocal laser microscopy (**c**). Scale bars, 20 μm. (**d**,**e**) Paraffin-embedded sections of peritoneum, from mice i.p. infected with NIH34 and skin from mice subcutaneously (s.c.) infected with NIH34 for 48 h (**d**), and of spleen and kidney from mice i.p. infected with or without K33 or NIH34 for 48 h, (**e**) were visualized with hematoxylin and eosin staining. The yellow arrows indicate the cells with ring-shaped nuclei. Scale bars, 100 μm. (**f**) Sorted IMCs were cultured with control medium (Med), G-CSF (50 ng ml^{-1}), M-CSF (10 ng ml^{-1}), GM-CSF (10 ng ml^{-1}), or IL-5 (10 ng ml^{-1}) for 2–4 days, and their absolute numbers were counted on the indicated days. Data are expressed as the average (mean ± s.d.) of triplicate wells ($n = 3$). The differences compared with Med were statistically significant ($^{**}P < 0.01$) as determined by Student's t-test. (**g**) γIMCs (blue line) and GM-CSF (2 days)-cultured γIMCs (GM2-γIMCs: red line) were stained for the indicated markers. Data are representative of three independent experiments. (**h**) Cytospin preparations of GM2-γIMCs were visualized with May-Grünwald-Giemsa staining. Scale bars, 20 μm. (**i**,**j**) γIMCs and GM2-γIMCs were cultured with erythromycin-treated NIH34 (MOI 100) in the presence of control rat IgG or an IFN-γ neutralizing mAb (clone R4-6A2) for 24 h. The levels of IFN-γ (**i**) and NO_2^- (**j**) in the culture supernatants were measured by ELISA and Griess reagent system, respectively. The average (mean ± s.d.) of triplicate wells is shown. Statistical significance ($^{**}P < 0.01$) was determined by ANOVA.

IFN-γ. Notably, the BMPC-derived unclassified granulocyte-lineage, such as γIMCs (but not immature PMNs), seems to appear during severe invasive GAS infections.

Distinction between γIMCs and MDSCs. MDSCs are composed of F4/80$^-$ or F4/80^{low} granulocytic MDSCs with ring-shaped nuclei, and F4/80$^+$ monocytic MDSCs[10,11]. They can produce IFN-γ[13]. Furthermore, granulocytic/monocytic MDSCs differentiate into CD11c$^+$ F4/80$^+$ Gr-1$^+$ cells[12], as do γIMCs (Fig. 5g). To identify the relationship between the types of γIMCs observed during severe invasive GAS infections and MDSCs, we investigated the ability of γIMCs to suppress T-cell responses. As reported previously, *in vitro*-differentiated Ly-6C$^+$ Ly-6G^{low} F4/80$^+$ MDSCs[9] spontaneously produced IFN-γ (Fig. 7a), and inhibited Ag-specific T-cell proliferation and IFN-γ production from T cells (Fig. 7b). Conversely, purified γIMCs failed to inhibit T-cell responses (Fig. 7c), suggesting that γIMCs are functionally distinct from MDSCs. Additionally, MDSCs markedly decreased in number and lost the ability to produce IFN-γ when cultured *in vitro* with severe invasive GAS isolates (Fig. 7a). Furthermore, CCR2$^-$ CX3CR1$^+$ CD31$^+$ γIMCs are phenotypically different from CCR2$^+$ CX3CR1$^-$ CD31$^-$ granulocytic MDSCs and CCR2^{high} CX3CR1$^-$ CD31$^+$ monocytic MDSCs (Supplementary

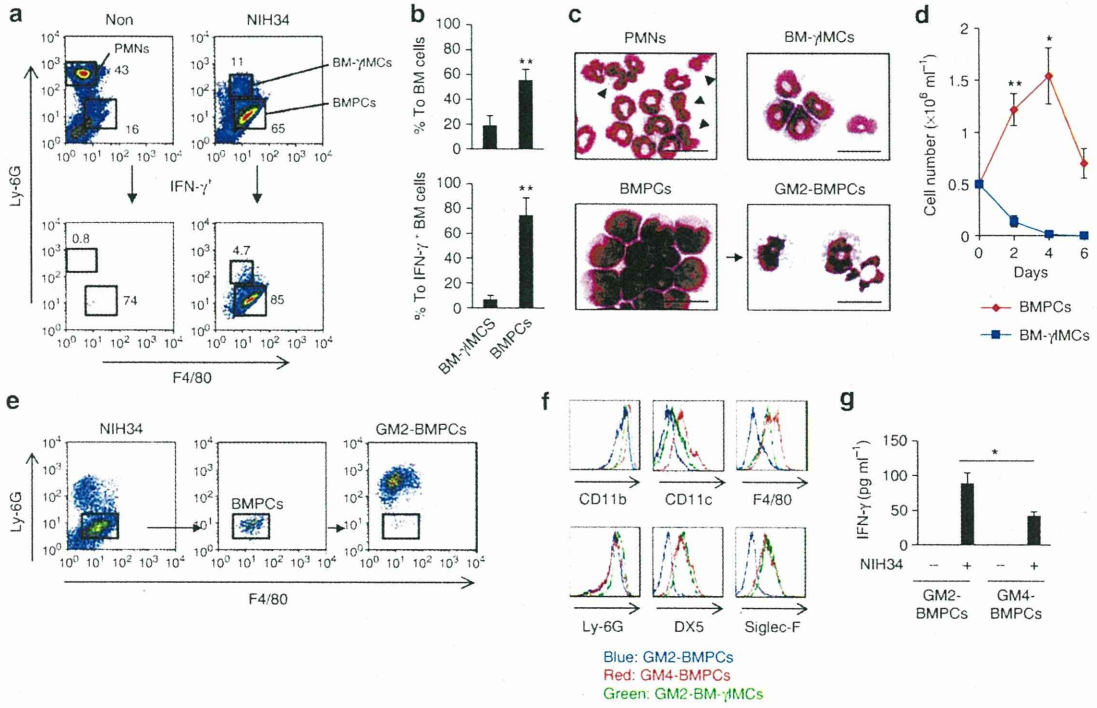

Figure 6 | BMPCs differentiate into γIMCs in the presence of GM-CSF. (**a**) C3H/HeN mice non-infected or i.p. infected with NIH34 (3.0×10^7 CFU per mouse) for 42 h were i.v. injected with monensin. Six hours later, the mice were killed and their bone marrow cells were immediately stained for the indicated markers, and analysed by ICS assay. Lower panels show the cells gated on the IFN-γ^+ population. The numbers (%) in the plots represent the proportion of PMNs, BM-γIMCs, and BMPCs to total (upper panels) and IFN-γ^+ (lower panels) bone marrow cells. (**b**) Proportion (%) of BM-γIMCs and BMPCs to bone marrow cells (upper panel) or IFN-γ-producing bone marrow cells (lower panel). Data are expressed as mean ± s.d. ($n=3$). The differences compared with the proportion of BM-γIMCs were statistically significant (**$P<0.01$) as determined by Student's *t*-test. (**c**) Cytospin preparations of sorted PMNs, BM-γIMCs, BMPCs, and GM-CSF (2 days)-cultured BMPCs (GM2-BMPCs) were visualized with May-Grünwald-Giemsa staining. Arrowheads indicate stab neutrophils or metamyelocytes. Scale bars, 20 μm. (**d**) Sorted BMPCs and BM-γIMCs were cultured with GM-CSF (10 ng ml^{-1}) for 2–6 days, and their absolute numbers were counted on the indicated days. Data are expressed as mean ± s.d. ($n=3$). The differences in proliferation increase were statistically significant (*$P<0.05$, **$P<0.01$) as determined by Student's *t*-test. (**e**) Flow cytometry profile of infected bone marrow cells (left), sorted BMPCs (middle), and GM2-BMPCs (right). Rectangles show a sorting gate of BMPCs. (**f**) GM-CSF-cultured BMPCs (2 days or 4 days; GM2-BMPCs, blue line; GM4-BMPCs, red line) and BM-γIMCs (2 days; GM2-BM-γIMCs, green line) were stained for the indicated markers. Data are representative of 3 independent experiments. (**g**) IFN-γ production from BMPCs. GM2-BMPCs or GM4-BMPCs were cultured with erythromycin-treated NIH34 (MOI 100) in the presence of control rat IgG or an IFN-γ neutralizing mAb (clone R4-6A2) for 24 h. The level of IFN-γ in the culture supernatants was measured by ELISA. The average (mean ± s.d.) of triplicate wells is shown. Statistical significance (*$P<0.05$) was determined by Student's *t*-test.

Table S1). Taken together, our results indicate that γIMCs, which appear in association with severe invasive GAS infections, comprise a novel subset of IFN-γ-producing cells, but not MDSCs.

Role of γIMCs in severe invasive GAS infections. To elucidate the protective role of γIMCs, we employed an adoptive transfer system using WT or *Ifng*$^{-/-}$ mice. CD11b$^+$ CD11c$^-$ F4/80^{low} Ly-6G$^+$ γIMCs were purified from the spleens of WT mice infected with severe invasive GAS at day 2, and transferred into recipient mice. These mice were infected with a lethal dose of severe invasive GAS isolates (5×10^7 CFU (high dose)/WT mouse, 1×10^7 CFU (low dose)/*Ifng*$^{-/-}$ mouse), and the bacterial loads (CFUs) in the blood were quantified. At 24 h post-infection, γIMC-recipients and IFN-γ-treated mice had significantly lower bacterial loads in the blood than did control mice (Fig. 8a–c). Additionally, all control mice and all IFN-γ-treated mice died. By contrast, 100% of high dose-infected WT recipients and low dose-infected *Ifng*$^{-/-}$ recipients of γIMCs, and also low dose-infected WT mice, survived until 60 h post-infection (Fig. 8d–f). Our results indicate that IFN-γ successfully improved the bacterial clearance, but that systemic IFN-γ treatment was detrimental to survival following GAS infections (Fig. 8a,c,d and f). Thus, it appears that γIMCs have a protective role in severe invasive GAS infections.

Discussion

Previous studies have indicated that T cells and NK cells may have a role in the production of IFN-γ during GAS infections[5,15–17,19–21]. In the present study, we have demonstrated for the first time that γIMCs in the peritoneal cavity, skin, spleen, kidney, peripheral blood and bone marrow (but not T cells or NK cells) produce IFN-γ *in vivo* during the early stage of severe invasive GAS infections. The intensity of IFN-γ production is comparable among γIMCs, T cells, and NK cells, but production by γIMCs takes place sooner than that by T cells and NK cells. Moreover, throughout the course of GAS infection, γIMCs are the main IFN-γ-producing cells in the spleen. We further observed that IFN-γ neutralized *Rag*$^{-/-}$ mice succumbed to severe GAS infection at a similar rate to WT mice. Taken together, our results indicate that γIMCs comprise the major source of IFN-γ during the early stage of severe invasive GAS infections, and that they have an important protective role.

Notably, IFN-γ administration reduced the number of bacteria in the blood, whereas the transfer of γIMCs, but not of IFN-γ,

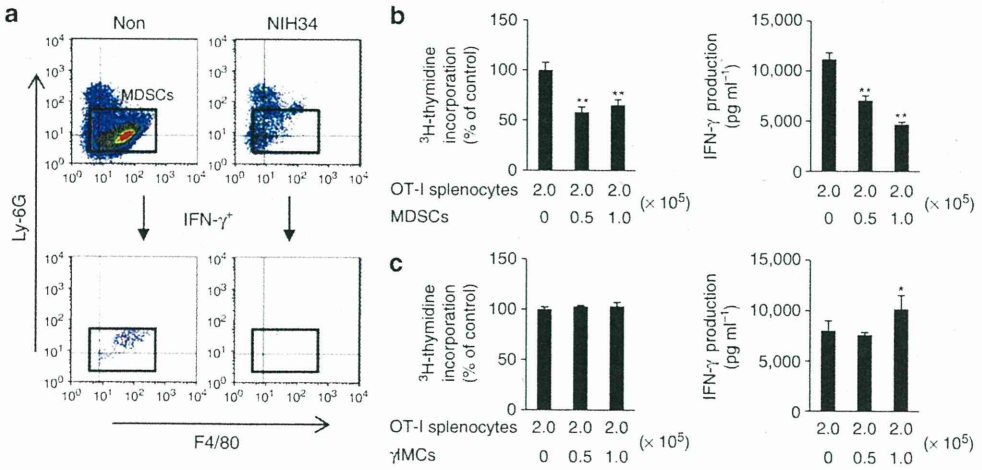

Figure 7 | γIMCs are functionally different from MDSCs. (**a**) C57BL/6 mouse bone marrow-derived MDSCs were differentiated *in vitro* with 40 ng ml^{-1} GM-CSF for 4 days. MDSCs were then incubated with or without severe invasive GAS isolates (NIH34; MOI 1) in the presence of brefeldin A (10 μg ml^{-1}). Three hours later, the cells were immediately stained for F4/80, Ly-6G, and IFN-γ, and analysed by ICS assay. Lower panels show the cells gated on the IFN-γ$^+$ population. (**b**,**c**) CD11b$^+$ CD11c$^-$ Ly-6C$^+$ Ly-6G^{low} *in vitro*-differentiated MDSCs, and CD11b$^+$ CD11c$^-$ F4/80^{low} Ly-6G$^+$ γIMCs, in the spleen from C57BL per six mice infected with NIH34 (3.0×10^7 CFU per mouse) for 48 h were isolated by FACS. Purified MDSCs (**b**) or purified γIMCs (**c**) were cultured at the indicated ratio with 2.0×10^5 splenocytes from C57BL/6 OT-I mice in the presence of antigenic $OVA_{357-364}$ peptides. Cell proliferation was measured using [^{3}H] thymidine uptake, and the level of IFN-γ in the culture supernatants was measured by ELISA. Each experiment was performed in triplicate. Mean ± s.d. is shown. The differences compared with OT-I splenocytes alone were statistically significant ($^*P<0.05$, $^{**}P<0.01$) as determined by ANOVA. Data are representative of three independent experiments.

improved the survival rate of mice following GAS infection. Therefore, IFN-γ was necessary, but not sufficient, to protect mice from severe invasive GAS infections. We propose that NO production from γIMCs (which is restrictively controlled by IFN-γ), perhaps combined with that from other myeloid cells, may have a critical defensive role during the early stage of infection. In systemic GAS infection, γIMCs are deployed in various infected tissues; thus, the derived IFN-γ, NO, and/or as yet unidentified protective factors may promote the development of innate immune responses for the activation of phagocytes. However, we were unable to exclude the possibility that excessive quantities of IFN-γ secreted by T cells following superantigens stimulation, by NK cells, and even by γIMCs at the late stage of infection, are detrimental to survival following GAS infections, by exacerbating inflammatory responses and organ injury.

γIMCs express phenotypic markers of the monocyte/macrophage and granulocyte lineages, and are phenotypically different from other Ly-6C$^+$ cells, such as inflammatory and resident monocytes[11,36]. Mature PMNs, immature PMNs, and their progenitors proliferate or maintain their survival in the presence of G-CSF[37]. By contrast, in the present study, γIMCs did not survive in the presence of G-CSF. However, in the presence of GM-CSF, they differentiated into a PMN-like phenotype. Thus, γIMCs are distinct from the PMN lineage that develops during steady-state haematopoiesis. In the presence of GM-CSF, γIMCs possessed the ability to express a specific marker for Eos, Siglec-F. Nevertheless, based on staining with H7 and T21, they were distinct from Siglec-F$^+$ splenic Eos. Our observation that γIMCs failed to proliferate in response to IL-5 are consistent with the previous finding that T21 mAb may recognize IL-5Rα and other myeloid cell surface protein(s)[38]. Thus, γIMCs are unlikely to be committed to an Eos lineage; similarly, they are phenotypically different from DX5$^+$ basophils and basophil lineage-committed progenitors[39].

Granulocytic MDSCs are very similar to γIMCs in terms of surface markers (CD11b, F4/80, Ly-6C, Ly-6G, CD44, CD49d, and CD62L)[10,11], dependency on a growth factor (GM-CSF)[12], and cytokine production profile (IFN-γ)[13]. However, in the present study, we reveal that MDSCs did not produce IFN-γ in response to *in vitro* GAS infections. This is consistent with the previous finding that MDSCs from septic mice did not produce IFN-γ[40]. MDSCs are believed to originate from, or be accelerated by, the blockade of normal haematopoiesis during chronic inflammation or in a tumour-bearing state. γIMCs and MDSCs may therefore be closely related cell populations, and their differentiation and function may be regulated by the host circumstances.

On the basis of our present findings, we conclude that γIMCs are committed to an unclassified granulocyte lineage with an immature phenotype, and that such cells have the potential to replenish granulocyte populations. Moreover, GM-CSF is essential for the extraordinary state, such as severe systemic infection, but not for normal haematopoiesis[41]. The replacement of GM-CSF-dependent γIMCs may be regarded as a marked shift to the left of the leukocyte differential, with many immature granulocytes in automated cell counting. This is a characteristic of severe invasive GAS infections in our mouse model and also in human diseases[4,28]. The role of γIMCs in other infections and inflammatory diseases remains to be elucidated.

In the present study, we reveal that γIMCs differentiate from a subpopulation of CD11b$^+$ CD11c^{low} F4/80$^+$ Ly-6G^{low} cells in the bone marrow; this is known as a monocyte lineage. No γIMCs were detected in *Ifng*$^{-/-}$ mice infected with GAS, and IFN-γ-producing BMPCs (but not γIMCs) failed to differentiate into granulocyte-like cells in the presence of an IFN-γ neutralizing mAb. These observations suggest that the generation of γIMCs depends on the production of IFN-γ by BMPCs themselves. IFN-γ derived from BMPCs and γIMCs may be a key component of haematopoiesis during innate and adaptive immune responses, as shown in cases of malaria and *Mycobacterium avium* infection[35,42]. In the steady state, a few IFN-γ-producing cells existed in the Ly-6C^{low} CD31$^+$ fraction, including mixed progenitors of bone marrow[43]. Thus, we cannot exclude the possibility that BMPCs exist in non-infected bone marrow and have potential to produce IFN-γ, and that a subset of bone marrow cells can produce IFN-γ for the reproduction of haematopoietic stem cells[42].

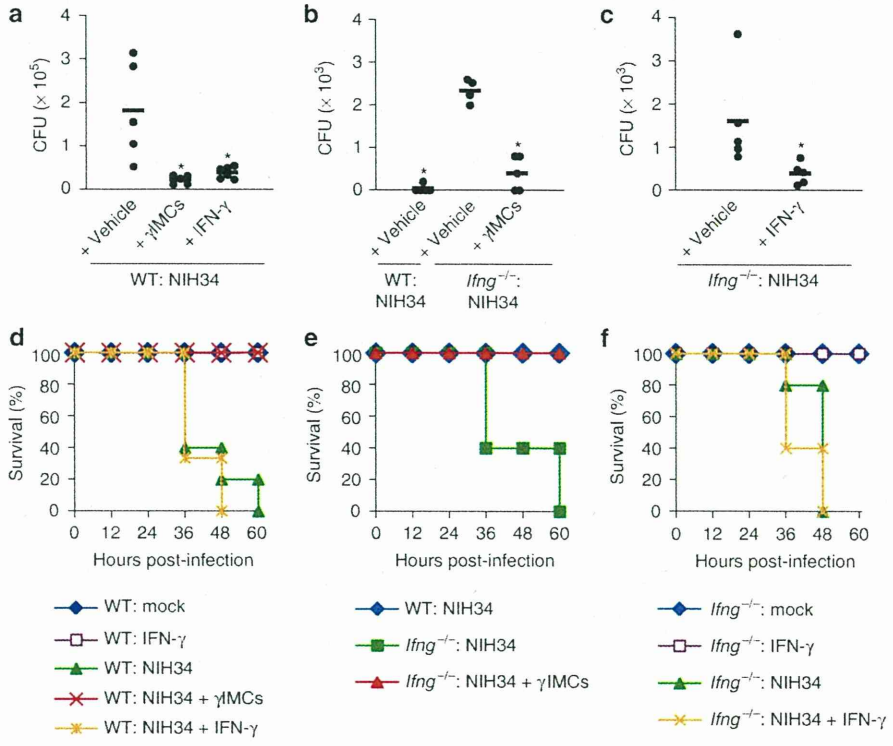

Figure 8 | γIMCs participate in protection against severe invasive GAS infections. (**a–f**) CD11b$^+$ CD11c$^-$ F4/80^{low} Ly-6G$^+$ γIMCs in the spleen from C57BL/6 WT mice infected with NIH34 (3.0×10^7 CFU per mouse) for 48 h were isolated by FACS. WT or *Ifng*$^{-/-}$ mice i.v. received 3.0×10^6 γIMCs, or were i.p. treated with IFN-γ (10 ng per mouse). (**a**,**d**) WT mice ($n=5$), WT recipients of γIMCs ($n=5$), and mice i.p. treated with IFN-γ ($n=6$) were i.p. inoculated with NIH34 (5.0×10^7 CFU per mouse). (**b**,**e**) WT mice ($n=5$), *Ifng*$^{-/-}$ mice ($n=5$), and *Ifng*$^{-/-}$ recipients of γIMCs ($n=5$) were i.p. inoculated with NIH34 (1.0×10^7 CFU per mouse). (**c**,**f**) *Ifng*$^{-/-}$ mice ($n=5$) and *Ifng*$^{-/-}$ mice i.p. treated with IFN-γ ($n=5$) were i.p. inoculated with NIH34 (1.0×10^7 CFU per mouse). (**a**,**b**,**c**) The CFU of NIH34 in the peripheral blood was determined at 24 h post-infection. The differences compared with NIH34-infected WT mice (**a**) or NIH34-infected *Ifng*$^{-/-}$ mice (**b**,**c**) were statistically significant ($^*P<0.05$) as determined by the Mann-Whitney *U*-test. (**d**,**e**,**f**) Survival was observed for 60 h post-infection. Data are representative of two independent experiments.

Ring cells are present in the blood and bone marrow of humans, especially patients with chronic myeloproliferative diseases[6–8] but only rarely in healthy control subjects[7]. Further investigations of peripheral blood leukocytes or bone marrow cells from severe invasive GAS patients are required, to clarify whether the human counterpart of γIMCs is a major source of IFN-γ in STSS patients.

PMNs are known to be essential for protection against non-invasive streptococcal infections. Following infection with severe invasive strains, PMNs are impaired by enhanced virulence factors (for example, streptolysin O)[18,27], and therefore other protective mechanisms are required for the recovery. The results of our present study indicate that γIMCs, a novel class of differentiated granulocytic ring cells, which comprise the major source of IFN-γ during the early phase of severe invasive GAS infections, may have an important role. During the later stage of infection, IFN-γ derived from T cells and NK cells may be detrimental to the host. Nevertheless, we believe that the orchestrated regulation of γIMCs serves as a protective mechanism against severe invasive bacterial infections.

Methods

Bacterial strains. The STSS criteria in this study are based on those proposed by the Working Group on Severe Streptococcal Infections[44]. The clinical isolates from STSS (NIH34 (*emm3* genotype], NIH230 (*emm49* genotype), NIH186 (*emm1* genotype), and NIH202-2 (*emm1* genotype)), and also from non-invasive infections (K33 (*emm3* genotype)), were collected by the Working Group for Beta-hemolytic Streptococci in Japan[18,27].

Mice. All work performed using mice was carried out in accordance with the guidelines for animal care approved by National Institute of Infectious Diseases. C3H/HeN and C57BL/6 mice (male, 5–6-weeks-old) were purchased from SLC. C57BL/6.*Rag1*$^{-/-}$ (ref. 26) and C57BL/6.*Ifng*$^{-/-}$ (ref. 45) mice were purchased from the Jackson Laboratory. All mice were maintained in a specific pathogen-free condition.

GAS infections in a mouse model. GAS were grown to late-log phase (OD_{600} = 0.75–0.95). Then, 1.0×10^7 CFU to 5.0×10^7 CFU GAS, suspended in 0.5 ml PBS, were i.p. inoculated into 6–8-week-old male mice. In some experiments, mice were i.p. administered with 1 mg of an anti-mouse IFN-γ neutralizing mAb (clone R4-6A2) or control rat IgG, or 10 ng of recombinant mouse IFN-γ (Wako Pure Chemical Industries) at infection. Plasma production of CXCL10 (an IFN-γ-inducible protein) at 24 h, after NIH34 infection, was used to assess the activity of inoculated IFN-γ (10 ng per mouse) in *Ifng*$^{-/-}$ recipients (*Ifng*$^{-/-}$ mice, 230.1 ± 58.2 pg ml^{-1}; IFN-γ-treated *Ifng*$^{-/-}$ mice, 468.2 ± 147.2 pg ml^{-1}*; C57BL/6 mice as positive control, 460.6 ± 126.9 pg ml^{-1}*). Data were expressed as mean ± s.d. ($n=5$). The differences compared with *Ifng*$^{-/-}$ mice were statistically significant ($^*P<0.05$) as determined by Student's *t*-test. Survival curves were compared using a log-rank test.

Measurement of cytokines in plasma. The plasma cytokine levels were determined by FlowCytomix (eBioscience) using a FACSCalibur flow cytometer (Becton, Dickinson and Company (BD)), according to the manufacturer's instructions.

Flow cytometry analysis. For the *in vivo* ICS assay[22,23], at day 2 post-infection, mice were intravenously (i.v.) injected with 500 μl of a PBS solution containing 100 μg monensin (Sigma-Aldrich) at 6 h before collecting. Splenocytes, peripheral blood cells, bone marrow cells, and leukocytes in the peritoneal cavity, kidney, and skin were collected and rapidly processed on ice. Single-cell suspensions were prepared, and red blood cells were removed using an ammonium chloride lysis buffer. For the *in vitro* ICS assay, non-infected or infected cells were cultured with 10 μg ml^{-1} brefeldin A (Sigma-Aldrich) for 3 h. One million cells were stained with Alexa Fluor 488-, FITC-, PE-, Alexa Fluor 647-, allophycocyanin (APC)-, or Pacific Blue-conjugated Abs (clones and suppliers, Supplementary Table S2) at 4 °C for 15 min. Nonspecific staining was blocked with an anti-mouse FcγR mAb (clone 2.4G2). Dead cells were excluded by 7-aminoactinomycin D (7-AAD; Sigma-Aldrich) staining. After washing, cells were fixed in 2% paraformaldehyde/PBS for 10 min and then permeabilized in 0.5% saponin/0.5% BSA/PBS (permeabilization